J. Microbiol. Biotechnol. (2009), **19**(9), 904–910
doi: 10.4014/jmb.0901.009
First published online 26 March 2009

JOURNAL OF MICROBIOLOGY AND BIOTECHNOLOGY

In Situ Single Cell Monitoring by Isocyanide-Functionalized Ag and Au Nanoprobe-Based Raman Spectroscopy

Lee, So Yeong[1], Soo Hwa Jang[1], Myung-Haing Cho[2], Young Min Kim[3], Keun Chang Cho[3], Pan Dong Ryu[1], Myoung-Seon Gong[4], and Sang-Woo Joo[3]*

[1]*Department of Pharmacology, College of Veterinary Medicine, Seoul National University, Seoul 151-742, Korea*
[2]*Department of Toxicology, College of Veterinary Medicine, Seoul National University, Seoul 151-742, Korea*
[3]*Department of Chemistry, Soongsil University, Seoul 156-743, Korea*
[4]*Department of Chemistry, Dankook University, Cheonan 330-714, Korea*

Received: January 6, 2009 / Accepted: February 16, 2009

The development of effective cellular imaging requires a specific labeling method for targeting, tracking, and monitoring cellular/molecular events in the living organism. For this purpose, we studied the cellular uptake of isocyanide-functionalized silver and gold nanoparticles by surface-enhanced Raman scattering (SERS). Inside a single mammalian cell, we could monitor the intracellular behavior of such nanoparticles by measuring the SERS spectra. The NC stretching band appeared clearly at ~2,100 cm^{-1} in the well-isolated spectral region from many organic constituents between 300 and 1,700 or 2,800 and 3,600 cm^{-1}. The SERS marker band at ~2,100 cm^{-1} could be used to judge the location of the isocyanide-functionalized nanoparticles inside the cell without much spectral interference from other cellular constituents. Our results demonstrate that isocyanide-modified silver or gold nanoparticle-based SERS may have high potential for monitoring and imaging the biological processes at the single cell level.

Keywords: *In situ* cellular imaging, nanoparticles, surface modification, Raman spectroscopy, cell monitoring

The ability to monitor the biological process within a cell could improve our understanding of cellular functions [2, 3, 19, 27]. Integrating nanoparticles and biological systems is changing diagnostics and therapy at the molecular and cellular levels. Recent developments of optical nanosystems and metal nanoprobes have received much attention for their potential application for taking intracellular measurements [34].

*Corresponding author
Phone: +82-2-8200434; Fax: +82-2-8200434;
E-mail: sjoo@ssu.ac.kr

Nanoparticles loaded with siRNA or anticancer drugs are being tested in the medical field against the specific genes involved in the pathogenesis of diseases or to increase the efficiency of drug delivery into the cells [25]. In addition, *in situ* cell monitoring is important for stem cell therapies since identifying the cell's origin of regeneration is critical for successful therapies. However, monitoring nanoparticles loaded with siRNA or therapeutic agents is difficult in an individual mammalian cell.

Silver and gold nanoparticles have attracted much attention in the past decade owing to their stability and optical properties [31]. Recent reports on the biological applications of silver and gold nanoparticles focus on the effects of size, shape, biocompatibility, uptake, and subcellular distribution of gold nanoparticles. Colloidal gold or silver nanoparticles are popular active platforms for surface enhanced Raman scattering (SERS) in most biological studies [28].

Since its discovery, SERS, as an ultra-sensitive spectroscopic tool for interface studies, has been widely used for biological sensing or molecular imaging near the surface of nanostructure assemblies [5, 6, 15, 30]. The analysis of spectral features has provided detailed information on surface reactions and the constituents of adsorbates. In principle, rather qualitative arguments concerning its intensified signals have been offered for data obtained *via* SERS, since it has been difficult to model real surfaces owing to the fact that both a long-range electromagnetic (EM) effect and a short-range chemical effect are assumed to simultaneously operate for overall enhancement. SERS on metal surfaces has shown great potential for use in biomedical analysis by introducing a mapping technique. A mapping stage with a submicrometer mechanical resolution may provide an image of live cells with detailed information about their cellular constituents.

The SERS method offers several advantages because it has different Raman signatures for high throughput screening

of various biomolecules with narrow bandwidths, avoiding spectral overlaps. SERS has been employed in cancer cell targeting and molecular imaging using thiolates [14, 17] or organic dyes [22]. Recent imaging of membrane proteins on cells has been demonstrated using a cyano-labeled SERS probe at ~2,200 cm^{-1} [9]. Although using SERS in live cell studies has gained increasing attention in recent years, most works conducted so far have focused on the detection of dye molecules introduced with silver particles [16].

There have been relatively few reports [1, 7, 8, 11–13, 18, 20, 24] exploring the chemisorption of organoisocyanides on metal surfaces. Aliphatic and aromatic diisocyanides are known to adsorb well on gold and silver *via* only one NC group, from a recent infrared and Raman spectroscopy study. The NC stretching region at 2,000–2,200 cm^{-1}, well isolated from interference from the many organic functional groups of proteins and DNA backbones between 300 and 1,700 cm^{-1} or 2,800 and 3,600 cm^{-1}, has the potential to monitor the location of the isocyanide-functionalized nanoprobes inside the cellular organism. In the present study, we report a novel experimental approach of cell imaging/monitoring that is able to evaluate the intracellular behaviors of the nanoparticles inside the single mammalian cell using isocyanide-modified silver and gold nanoparticles by means of SERS.

Materials and Methods

Materials

The citrate-stabilized gold nanoparticle was synthesized by following the procedures in the literature [21]. In a typical procedure, a 133.5 mg portion of $KAuCl_4$ (Aldrich) was initially dissolved in 250 ml of water (1.4 mM), and the solution was brought to the boil. A solution of 1% sodium citrate (25 ml) was then added to the $KAuCl_4$ solution under vigorous stirring, and boiling was continued for ca. 20 min. The resulting Au concentration, ignoring the evaporated water, should be 1.28×10^{-3} M and the concentration of the Au nanoparticles was estimated to be 9.1×10^{-9} M [20]. $AgNO_3$ (~90 mg) was dissolved in ~500 ml of distilled water, brought to the boil, and a solution of ~1% sodium citrate (10 ml) was added, and kept on boiling for ca. 1 h. 1,4-Phenylenediisocyanide (1,4-PDI, Fig. 1) (>95%) purchased from Aldrich was used without further purification. All the chemicals otherwise specified were reagent-grade, and triply distilled water of resistivity greater than 18.0 MΩ·cm was used in making aqueous solutions.

Table 1. Spectral data and vibrational assignment of 1,4-PDI[a].

Ordinary Raman	Ag SERS (~10^{-6} M)	Au SERS (~10^{-6} M)	Assignment[b]
In-Plane			
1,602	1,602	1,598	8a (A_1)
	1,508	1,510	19a (A_1)
1,194	1,200	1,211	9a (A_1)
1,171	1,163	1,166	7a (A_1)
Out-of-Plane			
	1,395		19b (B_1)
	1,321		3 (B_1)
Anchoring Group			
2,126	2,162	2,127	$\nu(N\equiv C)_{free}$
	2,172	2,193	$\nu(N\equiv C)_{bound}$

[a] Unit (Wavenumber).
[b] Based on ref. [7] in Wilson notation with symmetries based on the C_{2v} point group for the ring mode and ef. [7] for the isocyanide mode. The symmetry in the parenthesis corresponds to the C_{2v} point group.

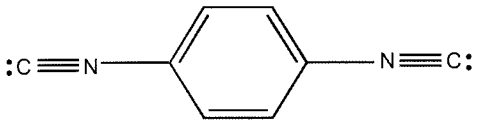

Fig. 1. 1,4-Phenylenediisocyanide (1,4-PDI).

Preparation and Characterization of Nanoparticles

The procedure of preparing Ag nanoparticles is reported to yield approximately 10^{11} particles/ml of homogeneously sized particles with a diameter of about 35 to 50 nm and an absorption maximum at ~400 nm [20]. The hydrodynamic diameters for Ag nanoparticles were measured to be 28 and 45 nm before and after the addition of 1,4-PDI, respectively. The transmission electron microscopy (TEM) images were obtained with a Tecnai F20 Philips microscope after placing a drop of colloidal solution on a carbon-coated copper grid. The TEM images of gold particles before and after adding 1,4-PDI are shown in Fig. 2. The elongated or polyhedra shapes may suggest an extensive aggregation or cross-linking between 1,4-PDI and gold particles [20]. The TEM image in Fig. 2B was obtained after at least a few hours had elapsed from the time of the addition of 1,4-PDI. The size and shape were not presumably due to the Ostward ripening process of the gold particles in themselves. UV–Vis absorption spectra of the colloidal solutions were obtained with a Shimadzu UV-3101PC spectrophotometer. The λ_{max} value of the UV–Vis extinction spectrum in the gold nanoparticles was found at 520 nm. The full width at the half maximum of the absorption peak was measured to be ~70 nm. The formation of 1,4-PDI-covered gold particles could be checked by a red shift to ~650 nm in a UV–Vis absorption spectrum or a decrease of interparticle distances in the TEM images. This may bring a strong resonance enhancement in SERS under our excitation wavelength at 632.8 nm.

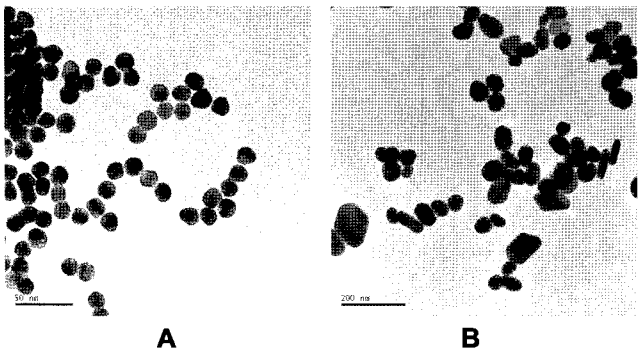

Fig. 2. TEM image of (**A**) pristine and (**B**) 1,4-PDI-modified Au nanoparticles.

Raman Spectroscopy

Raman spectra were obtained using a Renishaw Raman confocal system model 1000 spectrometer equipped with an integral microscope (Leica DM LM) [18]. Spontaneous Raman scattering was detected with 180° geometry using a Peltier cooled (-70°C) CCD camera (400×600 pixels). An appropriate holographic supernotch filter was set in the spectrometer for 632.8 nm. The holographic grating (1,800 grooves/mm) and the slit allowed the spectral resolution to be 1 cm^{-1}. The 632.8 nm irradiation from a 20 mW air-cooled HeNe laser (Melles Griots Model 25 LHP 928) with the plasma line rejection filter was used as the excitation source for the Raman experiments. Data acquisition time used in the Raman measurements was approximately 30 s. The Raman band of a silicon wafer at 520 cm^{-1} was used to calibrate the spectrometer. To obtain a mapping image, it took approximately 1 s to take a single Raman spectrum in a narrow region to take the N≡C bands centered at ~2,150 cm^{-1}. We could localize the specific points under our Raman microscope with a mapping stage. After focusing our laser beam into a certain point and obtaining the Raman spectrum, the sample was moved to the other local points using our custom-built mapping stage for *xy* translation with a submicrometer resolution [10]. The sample was moved by 1 μm after finishing each scan. The image was obtained from the ratios of the measured intensities at ~2,150 cm^{-1}. This Raman mapping image was compared with those using the ν_{8a} and ν_{7a} bands at ~1,600 and ~1,150 cm^{-1}, respectively.

To compare the Au or Ag nanoparticles labeled by Raman markers, we chose a simple molecule, 1,4-phenylenediisocyanide (1,4-PDI, Fig. 1) (>95%), purchased from Aldrich and used without further purification. The method in Raman measurements was described in a previous report [18]. 1,4-PDI-covered gold particles were fabricated by a self-assembly process. A concentrated ethanolic solution of 1,4-PDI was diluted into the aqueous gold nanoparticle solution. We initially prepared a 0.05 M ethanolic stock solution of 1,4-PDI and diluted the solution by a factor of 1,000. We then added this 1,4-PDI solution into the 1-ml gold nanoparticle solution with a 20-ml micropipette". The formation of 1,4-PDI-covered gold particles could be checked by a SERS spectrum.

Cell Culture

COS-7 cells [32] were cultured in Dulbecco's modified Eagle's medium (DMEM) (Invitrogen, Calsbad, CA, U.S.A.) supplemented with 5% fetal bovine serum (FBS) (Invitrogen, Calsbad, CA, U.S.A.) at 37°C in incubators supplied with 5% CO_2. For Raman spectroscopy measurement, the cells were plated into a nontreated 35-mm dish (SPL Life Sciences, Korea) at a density of 1×10^4 cells in DMEM containing 5% FBS. Next day, the cells were washed with phosphate-buffered saline (PBS) twice, and then 500 μl of nanoparticles was applied to the cells incubated within 500 μl of DMEM. After 3–4 days, the cells were monitored using Raman spectroscopy. After incubation, the cells were thoroughly washed with PBS and the cells were monitored using Raman spectroscopy.

RESULTS

A culture dish with sparsely distributed COS-7 cells was placed on the microstage in our Raman spectrometer at room temperature. The cells were washed twice with the phosphate buffer solution. An optical image was taken when the laser shutter was closed. Fig. 4 shows the SERS spectra at different local points of A, B, C, D, E, F, G, and H inside a single COS-7 cell after the uptake of the 1,4-PDI-modified Ag nanoparticles. The 1,4-PDI-modified nanoparticles were found not at the nucleus but in the cytoplasm. The Raman spectra for the A, D, F, G, and H spots do not contain the signatures of the vibrational bands of 1,4-PDI. For the "A" and "H" spots located outside the cell, the relatively weak bands were found at 1,000 and 1,030 cm^{-1}. These two bands can be ascribed to the C-C or C-N stretching band from the medium. In addition, the bands at ~1,600 and ~3,050 cm^{-1} could be assigned to the C-C and C-H bands, respectively, from the medium. Although not clearly shown, the Raman spectra at the "A" and "H" spots contained weak features at ~1,150 cm^{-1}. In contrast, the SERS spectra for the "B" and "E" spots contained quite prominent features of 1,4-PDI. The SERS spectra at the "C" spot revealed the characteristics of the cell's medium components and 1,4-PDI. It has to be admitted that the bands at ~1,150 or ~1,600 cm^{-1} may come not only from 1,4-PDI but also the cell's medium constituents. The ν(NC) band at 2,000~2,200 cm^{-1} should well represent the location of 1,4-PDI-modified nanoparticle probes instead. The red-shifted broad features at ~2,000 cm^{-1} in the Ag SERS spectra may be due to the cell and colloidal conditions in Fig 4. Fig. 4B exhibits an expanded view of the NC stretching region. For targeting, we checked whether the nanoparticles were delivered inside the cell's nucleus. As indicated in Fig 4, the Ag nanoparticles were supposed to be not inside the nucleus but in the cytosol. Fig. 5 shows the SERS spectra after the uptake of the 1,4-PDI-modified gold nanoparticles exhibited similar behavior to silver.

As recently reported for the cellular imaging [4, 29, 33], there are quite a few vibrational bands from amino acids

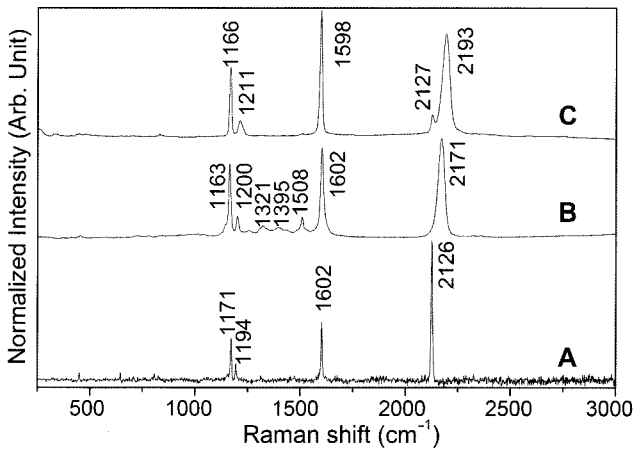

Fig. 3. (**A**) Ordinary Raman spectrum of 1,4-PDI. SERS spectra of ~10^{-6} M of 1,4-PDI on (**B**) Ag and (**C**) Au nanoparticles. The intensities are normalized for a better comparison.

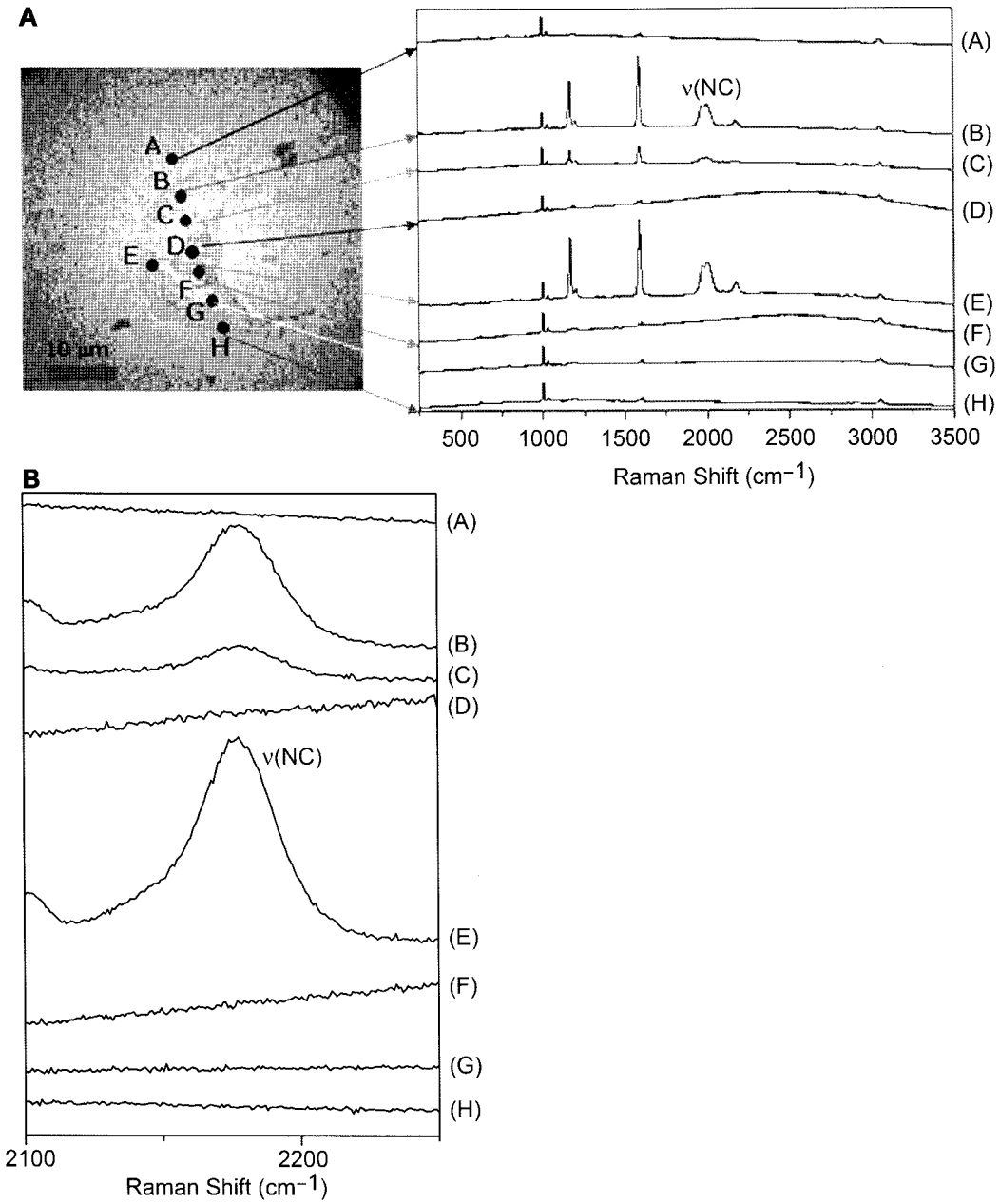

Fig. 4. A. SERS spectra at different local points of A, B, C, D, E, F, G, and H inside a single COS-7 cell after the uptake of the 1,4-PDI-modified Ag nanoparticles. The ν(NC) band uniquely indicated 1,4-PDI. **B**. An expanded view of the NC stretching region between 2,100 and 2,250 cm^{-1}.

and DNA backbones in the wavenumber region between 600 and 1,650 cm^{-1}. The C=O stretching band in esters is observed at ~1,750 cm^{-1}. The amide I, II, and III bands have been reported to be found at ~1,650, ~1,550, and ~1,250 cm^{-1}. In addition, the CH_3 and CH_2 stretching bands appear in the wavenumber region between 2,850 and 2,960 cm^{-1}. The NC stretching band at ~2,100 cm^{-1} should thus be well isolated from these congested regions and should better help locate the nanoparticles. As shown in Fig. 3, three prominent bands of the ν_{7a}, ν_{8a}, and ν(NC) bands appeared at ~1,150, ~1,600, and ~2,150 cm^{-1}, respectively, in the SERS spectra of 1,4-PDI. These three bands were comparatively used for the Raman imaging.

SERS Mapping Images

Fig. 6 compares the Raman mapping results when vibrational bands of 1,600, 2,150, and 1,150 cm^{-1} were used to image the cell. The brightest spot is the point where the band intensity is measured to be at its maximum. It seems that the mapping image with reference to the band at 2,150 cm^{-1}

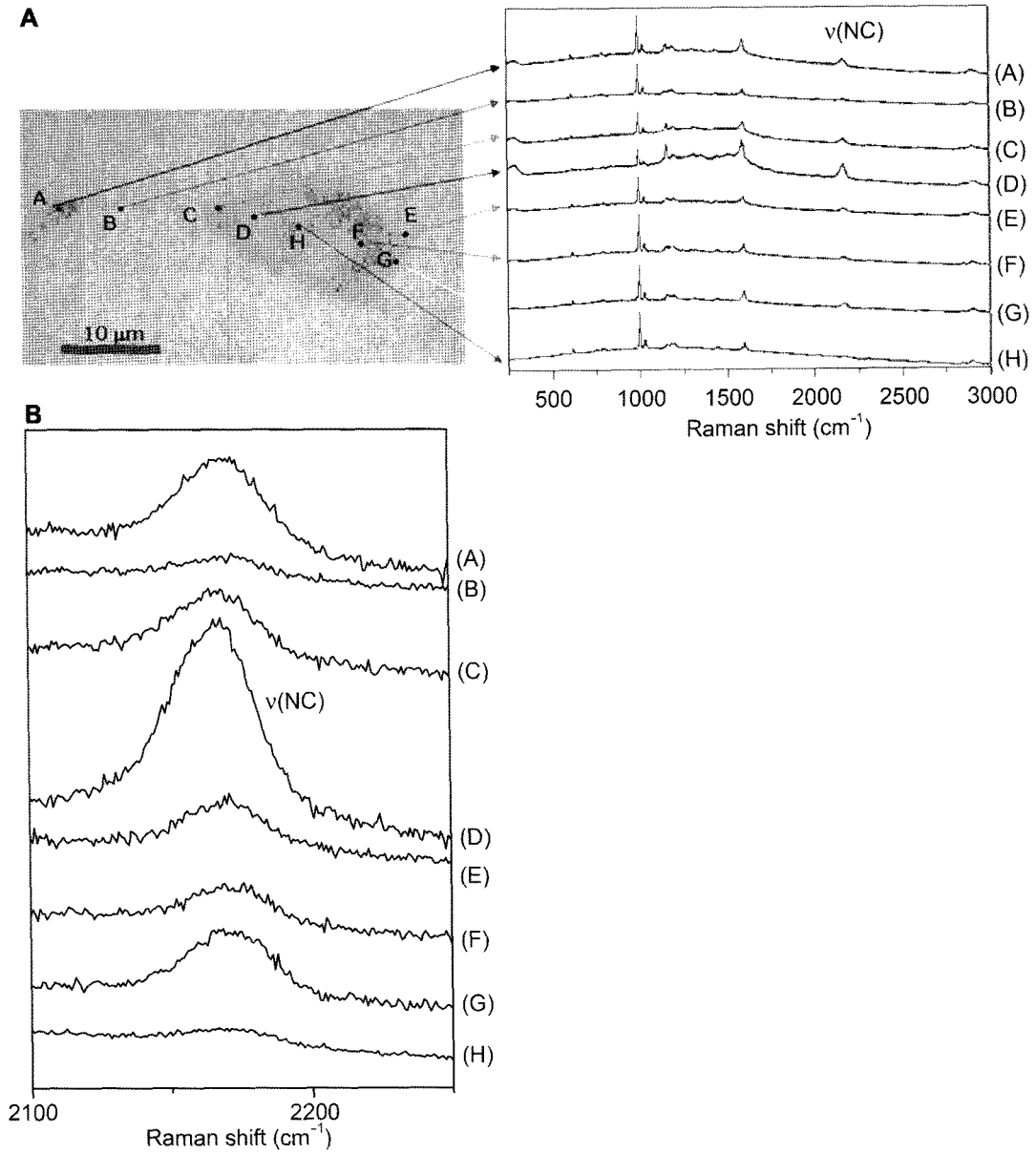

Fig. 5. A. SERS spectra at different local points of A, B, C, D, E, F, G, and H inside a single COS-7 cell after the uptake of the 1,4-PDI-modified Au nanoparticles. The ν(NC) band uniquely indicated 1,4-PDI. **B.** An expanded view of the NC stretching region between 2,100 and 2,250 cm^{-1}.

appeared to be better than those at 1,600 or 1,150 cm^{-1}. For the 2,150 cm^{-1} band mapping, the bright and dim areas were relatively well separated and discerned in comparison with those at 1,600 and 1,150 cm^{-1}. This may be due to the fact that quite a few bands such as DNA backbone, C-O stretching, C-C stretching, PO_2 stretching, C-O-H deformation, and C-O-C deformation could appear in this frequency region of 1,150 cm^{-1}. The ν_{8a} band at 1,600 cm^{-1} may also be possibly overlapped with the stretching bands of amino acids such as tyrosine and phenylalanine [33]. It is admitted that we cannot directly compare the mapping images for identical cells with reference to different vibrational bands because the cell appeared to be photodegraded after taking a Raman mapping image irradiated for a couple of hours. The vibrational mapping inside the single cell using the NC stretching band appeared to be advantageous, however, to those using the other bands after testing several individual cells.

Discussion

We examined the cellular uptake of isocyanide-derivatized Ag and Au nanoparticles in the mammalian COS-7 cell.

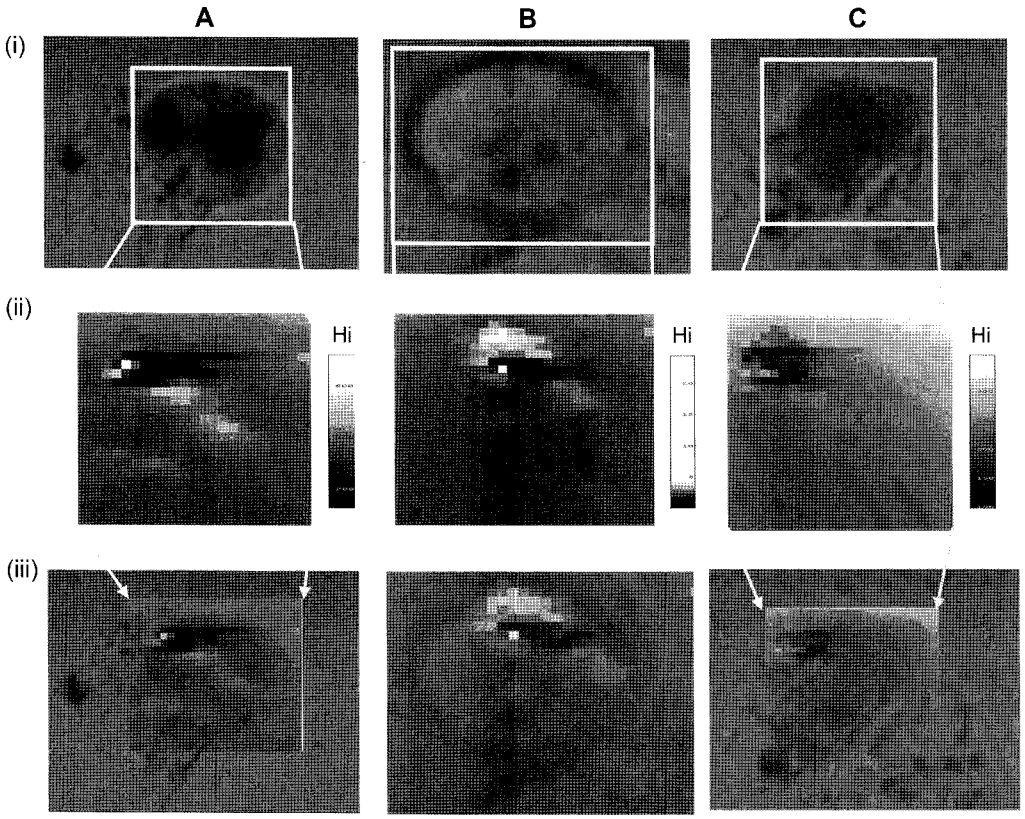

Fig. 6. Raman mapping of the COS-7 cell after the uptake of 1,4-PDI-modified Au nanoprobes using (**A**) 1,600, (**B**) 2,150, and (**C**) 1150 cm^{-1}, respectively, for the (i) bright optical image, (ii) Raman mapping image, and (iii) superimposed image of (i) and (ii). The rectangular areas denoting the scanned area in Figs. **A**, **B**, and **C** are 50 μm×50 μm, 60 μm×60 μm, and 50 μm×60 μm, respectively. The brightest spot is the point where the reference band intensity is measured to be at its maximum.

The ν(NC) band appeared to provide unique information on the presence and location of the cell without any interference from any organic constituents inside the single cell. Vibrational mapping using the NC stretching band at ~2,100 cm^{-1} inside the single cell appeared to be superior to those using the other bands at ~1,650 or ~1,150 cm^{-1}. Our result indicates that our experimental methodology can be utilized as a useful cellular imaging for *in situ* single cell monitoring. We also checked whether nanoparticles should be inside the cell, using a laser scanning confocal microscopy technique. Owing to the fluorescence quenching between the fluorescence tag Rhodamine 6G and metal nanoparticles, as in the previous report [23], it was difficult to discern the elucidated images. Our future research should achieve confocal resolution for cellular imaging without interference from the fluorescence quenching by choosing appropriate nanoparticles and tags. Under our experimental conditions, we could not achieve the resolution and sensitivity to obtain optical images for nanoparticles inside the cell. We are currently working on dark-field microscopy for imaging the metal nanoparticles [26]. We plan to use our SERS-based cell monitoring technique to target a specific protein inside various cells.

Acknowledgments

S.W.J. would like to thank Prof. Kwan Kim for helpful guidance. This work was supported by the Nano R&D program through the Korea Science and Engineering Foundation funded by the Ministry of Education, Science and Technology (2008-04308).

References

1. Bae, S. J., C.-R. Lee, I. S. Choi, C.-S. Hwang, M.-S. Gong, K. Kim, and S.-W. Joo. 2002. Adsorption of 4-biphenylisocyanide on gold and silver nanoparticle surfaces: Surface-enhanced Raman scattering study. *J. Phys. Chem. B* **106:** 7076–7080.
2. Bae, Y. M., K.-W. Park, B.-K. Oh, and J.-W. Choi. 2006. Immunosensor for detection of *Escherichia coli* O157:H7 using imaging ellipsometry. *J. Microbiol. Biotechnol.* **16:** 1169–1173.
3. Chanson, M., B. A. Kotsias, C. Peracchia, and S. M. O'Grady. 2007. Interaction of gap junction channels with other membrane channels and transporters. *Prog. Biophys. Mol. Biol.* **94:** 233–244.
4. Douglas, K. L., C. A. Piccirillo, and M. Tabrizian. 2008. Cell line-dependent internalization pathways and intracellular trafficking

determine transfection efficiency of nanoparticle vectors. *Eur. J. Pharm. Biopharm.* **68:** 676–687.
5. Eliasson, C., A. Lorén, J. Engelbrektsson, M. Josefson, J. Abrahamsson, and K. Abrahamsson. 2005. Surface-enhanced Raman scattering imaging of single living lymphocytes with multivariate evaluation. *Spectrochim. Acta Part A* **61:** 755–760.
6. Fleischmann, H., P. J. Hendra, and A. J. McQuillan. 1974. Raman spectra of pyridine adsorbed at a silver electrode. *Chem. Phys. Lett.* **26:** 163–166.
7. Han, H. S., S. W. Han, S. W. Joo, and K. Kim. 1999. Adsorption of 1,4-phenylene diisocyanide on silver investigated by infrared and Raman spectroscopy. *Langmuir* **15:** 6868–6874.
8. Henderson, J. I., S. Feng, T. Bein, and C. P. Kubiak. 2000. Adsorption of diisocyanides on gold. *Langmuir* **16:** 6183–6187.
9. Hu, Q., L.-L. Tay, M. Noestheden, and J. P. Pezacki. 2007. Mammalian cell surface imaging with nitrile-functionalized nanoprobes: Biophysical characterization of aggregation and polarization anisotropy in SERS imaging. *J. Am. Chem. Soc.* **129:** 14–15.
10. Joo, S.-W., J. K. Lim, and K. Cho. 2008. Resonance Raman process and photo-induced phase transition *via* 632.8 nm irradiation for diacetylene monocarboxylic acid derivative self-assembled layers on Ag surfaces. *Photochem. Photobio A* **194:** 356–361.
11. Joo, S.-W., W.-J. Kim, W. S. Yun, S. Hwang, and I. S. Choi. 2004. Binding of aromatic isocyanides on gold nanoparticle surfaces investigated by surface-enhanced Raman scattering. *Appl. Spectrosc.* **58:** 218–223.
12. Joo, S.-W., W.-J. Kim, W. S. Yun, and I. S. Choi. 2003. Adsorption of 4,4'-biphenyl diisocyanide on gold nanoparticle surfaces investigated by surface-enhanced Raman scattering. *J. Raman Spectrosc.* **34:** 271–275.
13. Joo, S.-W. and Y. S. Kim. 2004. Surface-enhanced Raman scattering study of benzyl mercaptide and benzyl isocyanide on gold and silver nanocolloid surfaces. *Coll. Surf. A* **234:** 117.
14. Jun, B.-H., J.-H. Kim, H. Park, J.-S. Kim, K.-N. Yu, S.-M. Lee, *et al.* 2007. Surface-enhanced Raman spectroscopic-encoded beads for multiplex immunoassay. *Comb. Chem.* **9:** 237–244.
15. Kneipp, K., A. S. Haka, H. Kneipp, K. Badizadegan, N. Yoshizawa, C. Boone, *et al.* 2002. Surface-enhanced Raman spectroscopy in single living cells using gold nanoparticles. *Appl. Spectrosc.* **56:** 150–154 .
16. Kneipp, J., H. Kneipp, K. Kneipp, M. McLaughlin, and D. Brown. 2008. Surface-enhanced Raman scattering for investigations of eukaryotic cells, pp. 243–261. *In* P. Lasch and J. Kneipp (eds.). *Biomedical Vibrational Spectroscopy.* John Wiley & Sons, New York.
17. Kim, J.-H., J.-S. Kim, H. Choi, S.-M. Lee, B.-H. Jun, Y. E. Kuk, *et al.* 2006. Nanoparticle probes with surface-enhanced Raman spectroscopic tags for cellular cancer targeting. *Anal. Chem.* **78:** 6967–6973.
18. Kim, S., K. Ihm, T.-H. Kang, S. Hwang, and S.-W. Joo. 2005. Binding property and structure of aromatic isocyanide self-assembly monolayers on Ag and Au surfaces. *Surf. Interf. Anal.* **37:** 294–299.
19. Kim, Y.-J., R. Neelamegam, M.-A. Heo, S. Edwardraja, H.-J. Paik, and S.-G. Lee. 2008. Improving the productivity of single-chain Fv antibody against c-Met by rearranging the order of its variable domains. *J. Microbiol. Biotechnol.* **18:** 1186–1190.
20. Lee, C.-R., S. Kim, C. J. Yoon, M.-S. Gong, B. K. Choi, K. Kim, and S.-W. Joo. 2004. Size-dependent adsorption of 1,4-phenylenediisocyanide onto gold nanoparticle surfaces. *J. Colloid Interface Sci.* **271:** 41–46.
21. Lee, P. C. and D. Meisel. 1982. Adsorption and surface-enhanced Raman of dyes on silver and gold sols. *J. Phys. Chem.* **86:** 3391–3395.
22. Lee, S., S. Kim, J. Choo, S. Y. Shin, Y. H. Lee, H. Y. Choi, S. Ha, K. Kang, and C. H. Oh. 2007. Biological imaging of HEK293 cells expressing PLCgamma 1 using surface-enhanced Raman microscopy. *Anal. Chem.* **79:** 916–922.
23. Li, H. and L. Rothberg. 2004. Colorimetric detection of DNA sequences based on electrostatic interactions with unmodified gold nanoparticles. *Proc. Nat. Acad. Sci. U.S.A.* **101:** 14036–14039.
24. Lin, S. and R. L. McCarley. 1999. Surface-confined monomers on electrode surfaces. Adsorption and polymerization of 1,6-diisocyanohexane on Au and Pt. *Langmuir* **15:** 151–159.
25. Lu, C.-W., Y. Hung, J.-K. Hsiao, M. Yao, T.-H. Chung, Y.-S. Lin, *et al.* 2007. Bifunctional magnetic silica nanoparticles for highly efficient human stem cell labeling. *Nano Lett.* **7:** 149–154.
26. McFarland, A. D. and R. P. Van Duyne. 2003. Single silver nanoparticles as real-time optical sensors with zeptomole sensitivity. *Nano Lett.* **3:** 1057–1062.
27. Nithipatikom, K., M. J. McCoy, S. R. Hawi, K. Nakamoto, F. Adar, and W. B. Campbell. 2003. Characterization and application of Raman labels for confocal Raman microspectroscopic detection of cellular proteins in single cells. *Anal. Biochem.* **322:** 198–207.
28. Patra, H. K., S. Banerjee, U. Chaudhuri, P. Lahiri, and A. Kr Dasgupta. 2007. Cell selective response to gold nanoparticles. *Nanomedicine* **3:** 111–119.
29. Rejman, J., V. Oberle, I. S. Zuhorn, and D. Hoekstra. 2004. Size-dependent internalization of particles *via* the pathways of clathrin- and caveolae-mediated endocytosis. *Biochem. J.* **377:** 159–169.
30. Schatz, G. C. and R. P. Van Duyne. 2002. Electromagnetic mechanism of surface-enhanced spectroscopy, pp. 759–774. *In* J. M. Chalmers and P. R. Griffiths (eds.). *Handbook of Vibrational Spectroscopy.* John Wiley & Sons, New York
31. Shipway, A. N., E. Katz, and I. Willner. 2000. Nanoparticle arrays on surfaces for electronic, optical and sensoric applications. *ChemPhysChem* **1:** 18–52.
32. Suh, J., D. Wirtz, and J. Hanes. 2003. Efficient active transport of gene nanocarriers to the cell nucleus. *Proc. Natl. Acad. Sci. U.S.A.* **100:** 3878–3882.
33. Tang, H. W., X. B. Yang, J. Kirkham, and D. A. Smith. 2007. Probing intrinsic and extrinsic components in single osteosarcoma cells by near-infrared surface-enhanced Raman scattering. *Anal. Chem.* **79:** 3646–3653.
34. Vo-Dinh, T., P. Kasili, and M. Wabuyele. 2006. Nanoprobes and nanobiosensors for monitoring and imaging individual living cells. *Nanomedicine* **2:** 22–30.